EUROPEAN FUSION DEVELOPMENT AGREEMENT

EFDA–JET–PR(03)54

R. Cesario, A. Cardinali, C. Castaldo, F. Paoletti, D. Mazon,
and JET-EFDA contributors

Modelling of Lower Hybrid Current Drive and Parametric Instability for High Performance Internal Transport Barriers of JET

Modelling of Lower Hybrid Current Drive and Parametric Instability for High Performance Internal Transport Barriers of JET

R. Cesario, A. Cardinali, C. Castaldo, F. Paoletti[1], D. Mazon[2],
and JET-EFDA contributors*

Associazione EURATOM-ENEA sulla Fusione, Centro Ricerche Frascati c.p. 65, 00044 Frascati, Italy
[1]*Princeton Plasma Physics Laboratory, Princeton, NJ, USA*
[2]*Association Euratom-CEA, CEA Cadarache 13108, St Paul lez Durance, France*
** See annex of J. Pamela et al, "Overview of Recent JET Results and Future Perspectives", Fusion Energy 2000 (Proc. 18th Int. Conf. Sorrento, 2000), IAEA, Vienna (2001).*

Preprint of Paper to be submitted for publication in
Physical Review Letters

ABSTRACT

A new extended modeling of Lower Hybrid Current Drive (LHCD) is presented. The model incorporates parametric instabilities (PI) of launched LH waves into a ray-tracing + Fokker Plank code providing robust and accurate simulations of the LH-driven current density profiles. The new approach is tested on the interpretation of the long lasting internal transport barriers (ITBs) of JET (Joint European Torus). The implementation of the results from the extended LHCD model in a transport code allows the simulation of the q-profile evolution in agreement with that provided by the Motional Stark Effect (MSE) reconstructed equilibria.. Low magnetic shear ($s \approx 0$) is produced by LHCD in a layer close to the ITB radial foot.

1. INTRODUCTION

The first long-lasting ITBs produced by Lower Hybrid Current Drive (LHCD) combined with the main heating power were produced in JET (Joint European Torus) with a moderate non-inductive current fraction (60%) [1-3]. A similar result has also been reproduced in JT60-U [4]. The experiments of JET indicated that a small LH-driven current fraction (30%) is deposited within a small radial region in the outer half of plasma close to the radial ITB foot, where low magnetic shear ($s \approx 0$) is produced [3]. The typical spatial and time behavior of the ITB, consisting in persistence for several seconds and large radial foot (at $\rho \approx 0.7$) [3], and the observed link between temperature, q-profiles and LHCD effects provide a crucial test for LHCD models. Such test has been performed for the present model, as shown below.

The LHCD is originated by the quasi-linear distortion of the electron distribution function produced by the propagating LH power $n_{//}$ spectrum ($n_{//}$ is the component of the wave refractive index parallel to the toroidal magnetic field) [5]. The present letter shows that a new model for LHCD profile based on spectral broadening due to Parametric Instability (PI) [6-12] results accurate and sufficiently robust under minor changes of the experimental profiles.

2. CALCULATION OF THE PROPAGATING $N_{//}$ SPECTRUM IN THE PRESENCE OF PARAMETRIC INSTABILITY

In order to interpret the LHCD experimental results [13], standard LHCD ray-tracing models utilize multi-radial reflections in toroidal geometry to bridge the existing $n_{//}$ gap between the launched spectrum and that of the absorbed wave. Such mechanism is justified only in case of weak absorption [14]. However, the most likely explanation of the velocity gap paradox are weak non-linearity of the parametric kind [14]. Including the non-linear plasma edge physics of PI in existing ray-tracing + Fokker Plank models [15], allows the consistent calculation of the launched LH wave $n_{//}$ spectral broadening. The PI analysis is implemented through the pump depletion modeling [6]. In this contest, the relevant parametric dispersion to be numerically solved is [7]:

$$\varepsilon(\omega,\mathbf{k}) - \frac{\mu_1(\omega_1,\mathbf{k}_1,\mathbf{k}_0,E_0)}{\varepsilon(\omega_1,\mathbf{k}_1)} - \frac{\mu_2(\omega_2,\mathbf{k}_2,\mathbf{k}_0,E_0)}{\varepsilon(\omega_2,\mathbf{k}_2)} = 0 \quad (1)$$

ε is the dielectric function, w indicates the complex frequency, $\boldsymbol{k}$ the wave-vector of the low frequency perturbation, the suffix i = 0,1,2, refers to the pump, the lower and the upper sidebands, respectively. The coupling coefficientsm $\mu_{1,2}$, referring to lower and upper sidebands, are calculated considering the ion magnetized **[8]**. In the plasma function, the sum over many (≈100) harmonics of the ion-cyclotron frequency is performed in order to achieve an accurate evaluation of the growth rate, which is given by the imaginary part $\gamma\ (\boldsymbol{k}_{1,\ 2,} E_0,\ \omega_0,\ \omega_{1,\ 2})$ of the frequency ω. The following selection rules for coupled modes hold: $\boldsymbol{k}_{2,1} = \boldsymbol{k} \pm \boldsymbol{k}_0,\ \omega_{Re2,1} = \omega_{Re} - \omega_0$, (the suffix "Re" denotes the real part). In the equation, the angle $\delta_{1,2} = \angle \boldsymbol{k}_{1,2\perp}, \boldsymbol{k}_{0\perp}$ is retained. Any angle value between group velocity of sideband and pump can be considered to properly account for the convective losses (in particular: $\delta_{1,2} \approx 0$, $k_{1,2y} \approx 0$, assuming $k_{0\perp} = k_{0x}$, $k_{0y} = 0$). The profiles of the homogeneous growth rate and of the real part of the frequency obtained through numerical solution of Eq. 1 are shown in **Fig. 1**. The plasma parameters of a typical LHCD-assisted ITB of JET [3] are utilized (see figure caption). Significant growth rates ($\gamma = 10^{-3}\omega_0$) for LH sideband waves with pump frequency shift $\omega \approx 10^{-3}\ \omega_0$ are observed. The ion-sound quasi-mode drives the instability ($\omega \approx k_{//}v_{Ti}$), which grows through both the lower and the upper LH sidebands ($\varepsilon_{Re1,2} \approx 0$), due to the small frequency shift by the pump wave **[10].** The uncertainty of the scrape-off density and temperature profile (up to a factor 3) determines the error bar on the growth rate profile. A variation of the edge input parameters within those uncertainties does not greatly affect the PI onset, but results in a small radial shift of the growth rate peak ($\Delta r \approx$ 1cm) within the scrape off layer. Comparable growth rates are obtained considering the plasma parameters of both the phases (preheating and main heating) in which the LHCD is performed. The PI phenomenon can affect different LHCD experiments due to the fact that the launched spectrum and the edge parameters need to occur in a same range ($n_{//0} \approx 2$, $\omega_{pe}/\omega_0 \geq 1$, $T_{eEdge} \approx 0.1$keV).

The convective nature of the instability has also been considered [6,7,10,16]. The threshold condition due to the finite spatial extent (L) of the pump requires the condition $\Gamma > 1$ for the spatial amplification factor $\Gamma = \gamma(\boldsymbol{k}_{1,} E_0,\ \omega_0,\ \omega_1)L/v_{g1\xi}$. In the formula, $v_{g1\xi}$ is the group velocity component of the sideband in the direction perpendicular to that of the pump. The characteristic scale ξ_d of the decay wave growth is given by $[\gamma\,(\boldsymbol{k}_{1,} E_0,\ \omega_0,\ \omega_1)/v_{g\xi},]^{-1}$. The power density threshold is exceeded over the whole scrape off layer. The sidebands have $n_{//}$ in the range: $n_{//} \approx 2.2 \div 3.0$. The amplification factor is maximizing for angle values $\delta_{1,2}$ in the range ≈ 3°÷20°, and reaches values in the range $\Gamma \approx 5 \div 12$ (Γ decreases with increasing $n_{//}$). The pump depletion depends exponentially on the amplification factor. The spatial amplification factor can be also written as: $\Gamma = x_0/x_d$, where x_0 is the distance in the radial direction a decay wave travels in one full pass across the pump wave region, and x_d is the characteristic scale length for the sideband growth, which depends on the pump wave potential ($x_d \propto \omega_0/k_0^2\Phi_0^2 v_{g0x}$). The distance x_0 has been calculated by ray-tracing of the pump and the sideband waves. Considering decay waves excited by the thermal noise, a fraction of about 10% of the pump power is deposited on sidebands with $n_{//} \approx 2.0 \div 2.3$. This fraction decreases at increasing $n_{//}$, due to the increase of the convective losses. For $n_{//} > 3.5$, no depletion occurs as the

RF power density goes below the convective threshold. In practice, the ray tracing acts as a low-pass filter in $n_{//}$ for the pump power depleted on the sideband, since the pump and sideband mismatch in wavenumber (and in frequency) increases at increasing $n_{//}$, thus determining a $n_{//}$ for pump depletion. After performing a ray tracing calculation for the different $n_{//}$ components of the spectrum launched by the antenna, a tail in the $n_{//}$ spectrum is produced by the PI. In the case of the aforementioned JET plasmas, the propagating $n_{//}$ spectrum after PI interaction is compared in **Fig. 2** with that launched by the antenna**.** About 15% of the launched LH power is depleted by LH sidebands with $n_{//}$ in the range from 2 to 3.5. Operation at higher densities or lower temperature at the edge increases both the growth rate and the $n_{//}$ cut-off for pump depletion. The line frequency broadening expected by PI activity (≈1MHz) is consistent with the past measurements collected with a radiofrequency probe during LH electron heating and CD experiments [9, 11, 12], including JET [17], which show a stronger broadening operating at high density (and high scrape-off density) as also is expected by the PI model.

3. MODELLING OF THE LH-DRIVEN CURRENT DENSITY AND Q PROFILES

The modeling is performed considering the plasma parameters of the main heating phase (at t = 6.5s, as in Figs. 1, 2), in which the LHCD-assisted ITB occurs. The use of the standard ray-tracing + Fokker-Plank model [15] requires two full ray passes and the observed LH deposition is not determined with acceptable precision. A variation of the input parameters within their uncertainties (i.e., density and temperature profiles (±10%) and the magnetic equilibrium (±20%)) results into a ≈ 50% uncertainty in the determination of the radial location of the deposition peak, as shown in **Fig. 3**. Similar results are obtained utilizing different LHCD ray-tracing (both 1-D and 2-D) codes [18,1,3]. Conversely, when the spectral broadening produced by PI is included in the extended model, full LH power at the first full pass is deposited in a narrow radial region of the outer half of plasma ($\rho \approx 0.7$). The deposition peak radius does not change significantly (≤10%) when variations of the input parameters within their uncertainties are considered.

A large broadening of the line frequency and LH power deposition at the periphery were typically found in LH heating and CD experiments operating at high plasma densities [9,11,12]. The present modeling is consistent with those results. Indeed, a larger spectral broadening and an LH power deposition more and more off-axis are predicted considering higher density at the edge and typical parameters of different LHCD experiments [16].

The q-profile evolution can be modeled by the JETTO code [19] supplemented by the LHCD model, considering the current profile produced by magnetic reconstruction in the early phase of discharge. A check is performed with the q-profile provided by EFIT conditioned by the MSE diagnostic [20], which is available at a time point (t = 4.45s) between the end of the LHCD pre-heating phase (at t = 4.0s) and before the switch-on of the LHCD power (at t = 5.8s) in the main heating phase (see Ref 1, 3 for further details of the operating conditions). The modeled and the MSE-q-profiles are compared in Fig. 4. Satisfactory agreement is found with the MSE-q-profile only when the spectral broadening is retained**.** The evolution of the modeled q-profile during the main heating phase (performed from t = 5s to 11s), shows that the q-value lies well inside the regions q = 3 and q = 2 during the whole LHCD-sustained ITB phase (from t = 5.5s to 9s). In addition, a layer with s ≈ 0 persists for several seconds in the outer half of plasma (at ρ ≈ 0.7). These features are expected to prevent the causes of the ITB collapse [21] and to stabilize turbulence [22], and are consistent with the aforementioned well assessed behavior of the LHCD-assisted ITB. Conversely, without LHCD performed during the main heating phase, the q evolves more rapidly and the s ≈ 0 layer moves inwards consistently with the advanced ITB collapse (occurring at the onset of a q = 3 snake) [1,3]. When the spectral broadening is retained, a better simulation can be performed of both loop-voltage and internal inductance. The residual electric field, the fraction of non-inductive current (≈ 60%), and an effective ion charge (≈ 2.4) have been considered in the present analysis.

CONCLUSIONS.

The small (≈ 15%) LH pump power depletion accompanying some broadening of the launched $n_{//}$ spectrum is sufficient to determine the LHCD profile when the edge physics of parametric instability is included in an extended ray-tracing + Fokker-Planck code. The modeling is successfully tested utilizing typical parameters of the long lasting ITBs of JET. Those configurations were obtained through the application of a small LHCD fraction (≈ 30%), thus indicating that the magnetic shear is being locally and efficiently modified, as expected by the present model. The use of the results from the extended model in a transport code allows simulations robust against uncertainties in plasma parameters of the q-profile evolution and in agreement with the diagnostics' measurements. A layer with low magnetic shear is expected to occur in the outer half of plasma, consistently with both the location of the ITB radial foot and with the ITB time duration. The spectral broadening interests different LH experiments. It allows explaining the more and more off-axis deposition found in the LH heating and CD experiments when operating at high edge density. Conversely, operation with low recycling/higher electron temperature at the edge, e.g., via high plasma current or Litium-coating of the vessel [23, 24], are recommended for reducing the PI growth and, consequently, for enhancing the plasma density limit of the LHCD operation.

Utilizing only the multi-radial reflections to bridge the $n_{//}$ gap, as performed in standard LHCD models, is not sufficient for modeling the experimental ITB results with sufficient accuracy. The use of the proposed extended LHCD model as a predictive tool will allow the design of experimental scenarios where LHCD will be used to control the q-profile, as required for improved stability and confinement in advanced-tokamak regimes.

ACKNOWLEDGEMENTS

The authors acknowledge F. Santini, Drs Y. Baranov, C. Challis, X. Liatudon, J. Mailloux' and A. Tuccillo for the helpful discussions, and L.M. Carlucci for her editorial comments.

REFERENCES

[1]. J. Mailloux, B. Alpmer, Y. Baranov, et al., Phys. of Plasmas, Vol. 9 No. 5 May 2002
[2]. F. Crisanti, X. Litaudon, J. Mailloux, et al., Phys. Rev. Lett., April 2002
[3]. C. Castaldo, R. Cesario, A. Cardinali, et al., Phys. of Plasmas, Vol. 9 No. 8 August 2002
[4]. S. Ide, et al., at PPCF Nov. 2002
[5]. N.J. Fisch, Rev. Mod. Phys, **59**, (1987), 175
[6]. C.S. Liu in Advances in Plasma Physics, Edited by A. Simon and W.B. Thomson, (Wiley, New York 1976) Vol. 6 p. 121
[7]. L. Chen, R. and L., Berger, Nucl. Fusion **17** 779 (1977)
[8]. V.K. Tripathi, C.S. Liu and C. Grebogi, Phys. Fluids **22** 1104 (1979)
[9]. M. Porkolab, Y. Takase, et al. Phys Fluids 1985
[10]. C.S. Liu and V.K. Tripathi Phys. Fluids Report 24 1709 (1984)
[11]. R. Cesario and A. Cardinali, Nucl. Fusion 29, n.10 (1989) 1709
[12]. R. Cesario, et al., Nucl. Fusion, **32**, 2127 (1992)
[13]. P.T. Bonoli, R.C. Englade, Phys. Fluids, 29 (1986) 2937
[14]. M. Brambilla, Kinetic Theory of Plasma Waves, Clarendon Press, Oxford 1998, p. 551-552, p. 557
[15]. A. Cardinali, in Recent Results in Phys Plasmas, 1, 185, 2000
[16]. R. Cesario, et al, submitted to PoP
[17]. A. Ekedahl et al. EPS 1996; V. Pericoli-Ridolfini et al., Plasma Phys. Contr. Fus. 39 (1997) 1115
[18]. A.R. Esterkin and A.D. Piliya, Nucl. Fusion **36** (1996) 1501
[19]. G. Cenacchi, A. Taroni, in Proc. 8th Computational Physics, Computing in Plasma Physics, Eibsee 1986, (EPS 1986), Vol. 10D, 57
[20]. N. Hawkes, et al., PRL 2001
[21]. C. Challis et al. PPCF 2001
[22]. F. Romanelli, F. Zonca, Physics of Fluids B, **5**, 4081-9, (1993)
[23]. M. Abdou, et al., Fus. Eng. Des. 54 (2001) 181
[24]. S.I. Krasheninnkov, L.E. Zakharov, G.V. Pereverzev Phis. of Plasmas 10 1678 (2003)

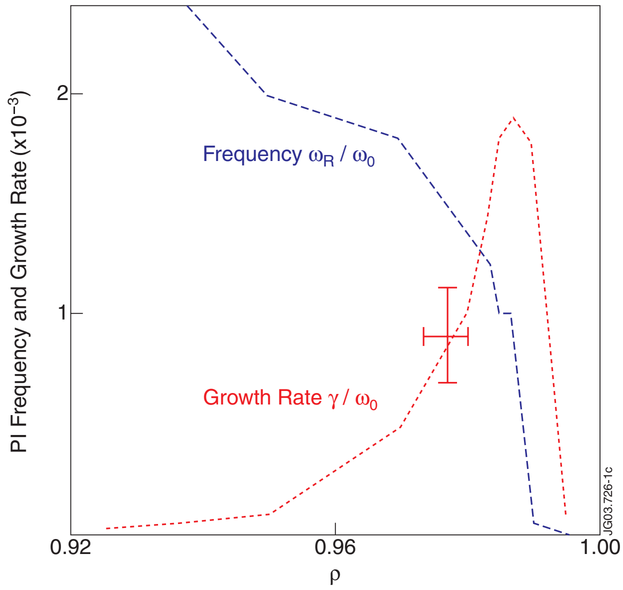

*Figure 1: Profiles of the homogeneous growth rate and of the real part of the frequency obtained by solving the parametric dispersion relation (Eq. 1). The following plasma parameters of the JET Pulse No: 53429 at a time point (at t = 6.5s) during the main heating phase are considered. B_T = 3.4T; I_P = 2.3MA, $<n_e> \approx 2\ 10^{19} m^{-3}$; LH power = 2MW; frequency = 3.7 GHz; $n_{//}$ spectrum with peak $n_{//0}$ = 1.8 and width = 0.43; antenna dimensions: a_y = 0.84m, **a_z=0.16m;** local toroidal magnetic field $B_T \approx 2.6T$. Plasma edge parameters (between the antenna mouth and the separatrix): scrape-off radial dimension: ≈ 5cm, density: $n_e = 0.2 \div 2 \cdot 10^{18} m^{-3}$, temperature: $T_e = 50eV \div 700eV$, electron-ion temperature ratio: $T_e/T_i = 1 \pm 0.5$.*

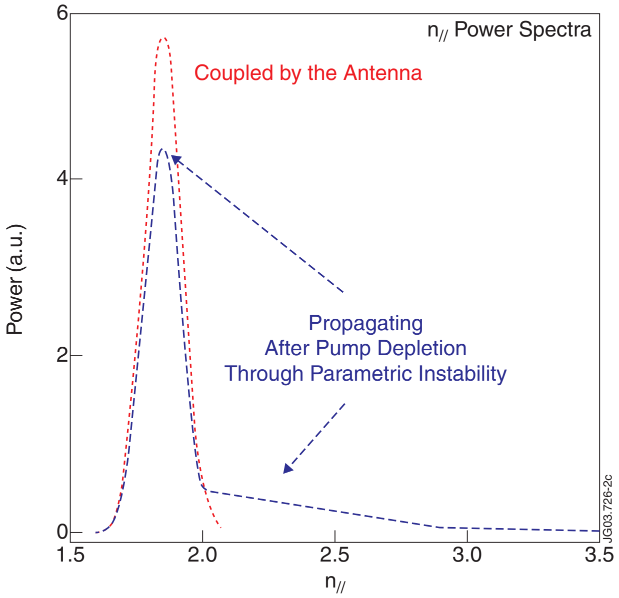

Figure 2: LH $n_{//}$ power spectrum produced by the pump depletion (≈ 15%) through parametric instability (PI) driven by ion-sound quasi-mode. The $n_{//}$ spectrum launched by the LHCD antenna is shown for comparison. Plasma parameters as in Fig. 1.

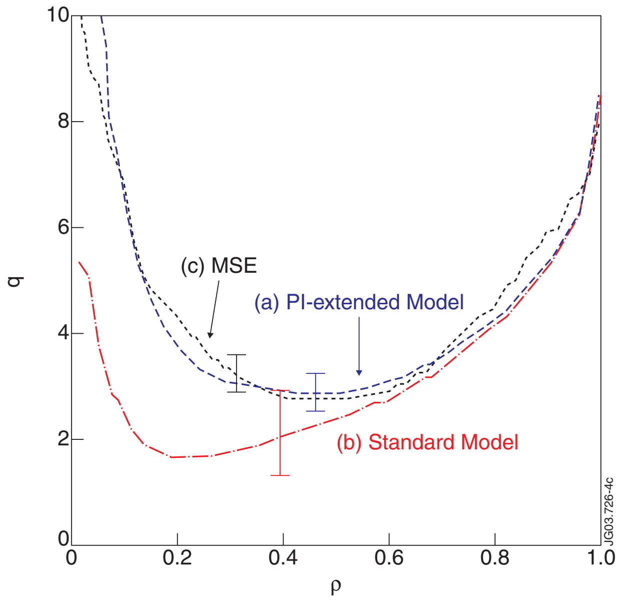

Figure 4: i). Plasma parameters as in Fig. 1. ii). Comparison of the q-profile modeled by the JETTO code with inputs from the PI-extended LHCD code, at the same time point (t = 4.45s) of the available MSE q-profile (a) including the PI effect, (b) neglecting the PI effect , (c) MSE q-profile.

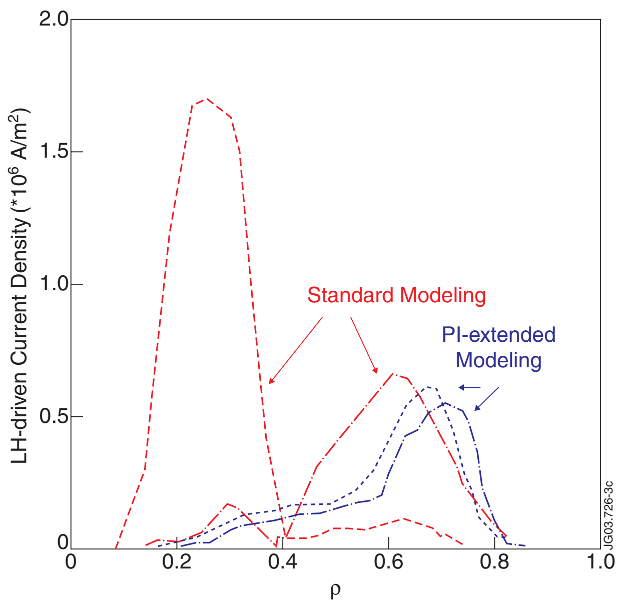

Figure 3: Comparison of the modeled LH-driven current density profile for the LHCD-assisted ITB of JET during the main heating phase (at t = 6.5s). The dashed and dashed-dotted curves correspond to two results obtained using the standard modeling while considering the input experimental kinetic and magnetic reconstruction profiles at the extremes of their error bars. The dotted and dashed-double dotted curves are obtained in a similar way, but utilizing the PI-extended model. Plasma parameters as in Fig. 1.